

Catalytic Properties of Pd₇₀Co₂₀Mo₁₀ and a Comparison of its Experimental and Theoretical Structure

M. Garza Castañón¹, O.V. Kharissova*¹, M.A. Jiménez¹ and S. Velumani²

¹Facultad de Ciencias Físico-Matemáticas, UANL, Monterrey, México, Pedro de Alba S/N, Ciudad Universitaria, C.P. 66450, San Nicolás de los Garza, N.L. México

²Instituto Tecnológico y de Estudios Superiores de Monterrey – campus Monterrey, México

Abstract: Results obtained by computer modeling and simulation using *ab-initio* and molecular dynamics techniques for elucidation of structural and catalytic properties of the PdCoMo trimetallic compound are reported; a comparison of these results with those obtained by sputtering deposition onto a nafion membrane to be used as catalyst for a 1KW PEM fuel cell is made. Structure was calculated by *ab-initio* methods and experimentally determined by XRD and AFM techniques. Catalytic properties were calculated by *ab-initio* and molecular dynamics techniques, and experimentally determined directly on a 1 KW PEM fuel cell.

Keywords: PEM fuel cell, trimetallic catalyst, MEA.

INTRODUCTION

Fuel cells have been widely studied [1-10] in the last decades, since they represent a clear path to produce electric energy. Of particular interest is the case of the proton exchange membrane (PEM) fuel cells, due to their high-power densities and relatively low operation temperatures from 55 to 80 °C. Several approaches have been done to develop low-cost, high performance[11-19] PEM fuel cells membranes, improvement of the electrodes [20-23], modeling [24-26] and instrumentation techniques [27-30]. These approaches involve efforts as improving membrane-electrodes assemblies (MEAs) [31-34], development of composite catalysts to improve the CO-tolerance of the fuel cell, fuel reforming, etc. The purpose of this work is to show results obtained for a MEA prepared by depositing carbon support directly on the nafionTM membrane by electric arc technique, and deposit Pd-Co-Mo trimetallic compound as anodic and cathodic catalysts synthesized at the nanoscale to increase the catalytic surface of the MEA. Background work involves the use of computational *ab-initio* techniques to develop an atomistic model (crystal lattice) for the trimetallic compound, calculate its XRD pattern to validate the model, its hydrogen dissociation reaction capability through the calculation of the transition state (TS) structure and enthalpy, and compare with other two Pd-based trimetallic compounds.

MATERIALS AND METHODS

A 2.4 GHz, 200 GB PC was used for the calculations. The software was Materials StudioTM with its Reflex (XRD simulation) and CASTEP modules.

a) Raw Materials

For the synthesis of the nanostructured catalysts, a Pd-Co-Mo (70:20:10 %) target of size 2" diameter and 0.250"

thickness was used. As proton exchange membrane, a 50X50 mm sized Nafion 112TM membrane was used (Dupont). Graphite 7-mm bar was used as the anode and cathode for the electric arc equipment to be deposited as the catalyst's support.

b) Equipment

For the carbon support deposition, a JEOL JEE-400 vacuum evaporator was used. To synthesize catalytic nanoparticles by inert gas condensation (ICG), the technique a Nanosys 500 ultra-high-vacuum system (Mantis ltd.) was used. To characterize structure, a D-5000 (Siemens) X-ray diffractometer was used. Morphology was checked by TEM, and particle size was characterized by AFM non-contact technique. Elemental analysis was carried by Auger spectroscopy (AES) technique to compare between target's and nanoparticles deposit composition. Electrochemical characterization was carried out directly in a 1-KW PEM fuel cell stack.

THEORETICAL CALCULATIONS

Using a CASTEP (Cambridge Serial Total Energy Package) module, an atomistic model which will simulate the crystal lattice of the real compound accomplishing both the chemical composition and XRD pattern was developed for the Pd₇₀Co₂₀Mo₁₀ compound. For comparison, experimental XRD pattern for Pd-Co-Mo is taken from the target, and Scherrer's formula was considered to calculate the lattice parameter and build up the atomistic model. To assure the correct description of the structure, a simulation of the XRD diffraction pattern was run using the Reflex module of Materials StudioTM software. The simulated diffractometer was set to X-Ray, Copper K α source, with a wavelength of 1.54056 Å.

Calculation of the hydrogen dissociation reaction, widely studied for metallic systems [35-39], was done through the transition state (TS) structure estimation, which has been reported to be a very valuable tool to analyze molecule-simple/complex-solid interactions [40]. The TS structure is defined as the steady point where the energy is maximum in

*Address correspondence to these authors at the Facultad de Ciencias Físico-Matemáticas, UANL, Monterrey, México, Pedro de Alba S/N, Ciudad Universitaria, C.P. 66450, San Nicolás de los Garza, N.L. México; E-mail: okhariss@mail.uanl.mx

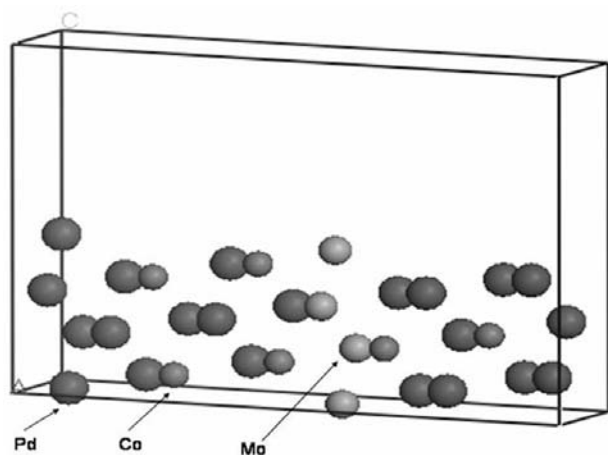


Fig. (1). Atomistic model for Pd-Co-Mo (70:20:10 %) compound.

the direction of the reaction path. During a chemical reaction, the total energy of the reactants will change. It will increase up to a maximum level known as the “activation energy”, then decrease down to the product energy. A GGA-RPBE functional was set, and calculation was carried only for the gamma point to optimize calculation time.

EXPERIMENTAL

XRD was taken for the target, in order to have a comparison with the nanoparticles produced and the atomistic model developed with the use of Materials Studio software. The Siemens D-5000 diffractometer was set to a 35 KV po-

tential, 25 mA current with a CuK α ($\lambda = 1.5406 \text{ \AA}$) anode and a W filament, with a Ni secondary monochromator. The step time was set to 1.1 sec, the step size used was 0.05° , scan angles were fixed from $2\theta = 5^\circ$ to 90° . Rotation was set to 15 RPM.

Hydrophobic carbon (graphite) was deposited on the Nafion 112 membrane on both faces using the JEE-400 vacuum evaporator. Vacuum pressure was set to 4×10^{-3} Pa. Distance from electrodes to membrane was fixed to be 150 mm, since temperature rise during the electric arc generation may lead to burn the membrane. Deposition time was 5 seconds. Pd-Co-Mo 3-nm particles were deposited on the carbon-covered membrane. Ultra-high-vacuum pressure was set to 4.3×10^{-8} torr. Condensation zone was set to 92 mm, with an Ar and He flow of 10 and 20 sccm. Membranes were prepared by this method, with deposition time of 8, 15 and 30 minutes.

RESULTS AND DISCUSSION

An atomistic model is developed for Pd-Co-Mo compound that satisfies both structure and chemical composition (70:20:10 %). Fig. (1) shows the atomistic model for this compound, where the crystal is created starting from the experimental data reported by Raghuv \ddot{e} r *et al.* [41], positions of the atoms were estimated to accomplish chemical composition and XRD pattern. Fig. (2) shows comparison between experimental (a) and calculated (b) XRD pattern, as can be clearly seemed, experimental pattern taken from the sputtering target and simulated XRD pattern match in a highly reliable way. From the Scherrer's equation (1.1) a crystallite

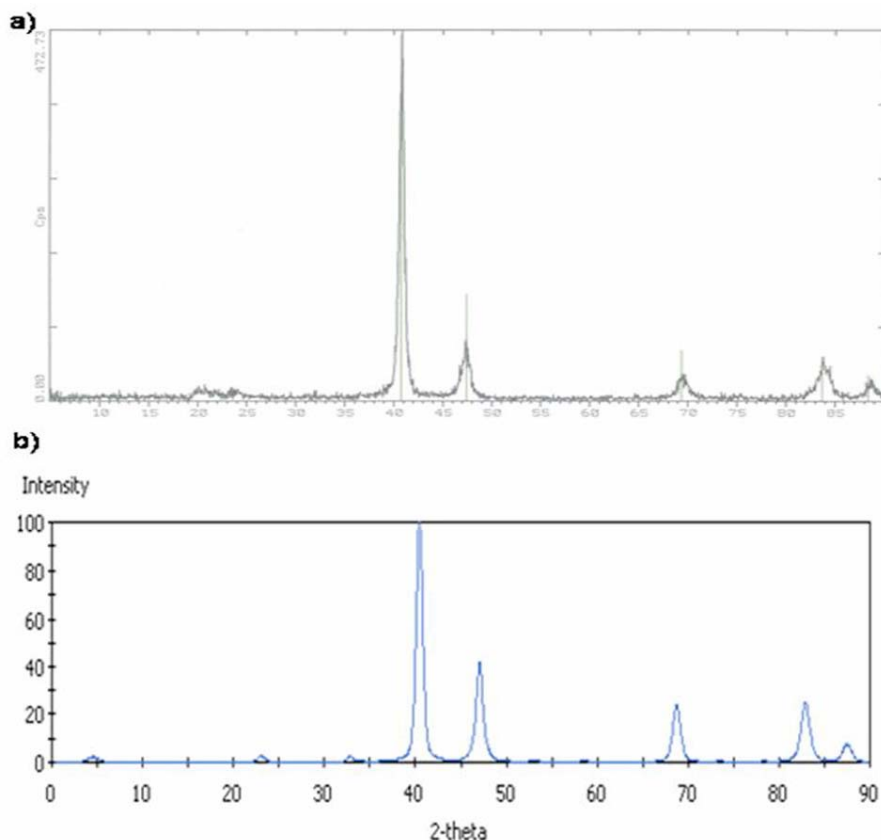


Fig. (2). Pd-Co-Mo XRD pattern: (a) experimental, (b) calculated.

Table 1. Reaction Energies for H₂-Metal (111) Surface

Metal	Reaction energy (eV)
Pt	-0.591
Pd-Co-Au	-0.531
Pd-Co-Mo	-0.396
Pd-Co-Ni	-0.238

size is estimated to be 48.2 nm, and simulated XRD pattern and structure are refined to fit the experimental data.

$$\Delta(2\theta)_{hkl} = \frac{180\lambda}{(\pi L_{hkl} \cos \theta)} \quad (1.1)$$

where:

$$\Delta(2\theta)_{hkl} = \text{FWHM in the direction } hkl$$

$$\lambda = \text{X-ray wavelength (1.5406 \AA)}$$

$$L_{hkl} = \text{crystallite size in the direction } hkl$$

$$\theta = \text{diffraction angle}$$

TST calculation results give reactions energies shown in Table 1. Lower enthalpy will result on a higher probability of hydrogen dissociation by the metal. Comparison is done with other two Pd-based trimetallic compounds and with pure Pt showing that Pd-Co-Au composite exhibits the most negative enthalpy for the hydrogen dissociation reaction. Since purpose of this work is to develop a low-cost catalyst,

Pd-Co-Mo is chosen to accomplish the requisite of a non-precious-metal catalyst.

Nanoparticles were synthesized by the Nanosys 500. Fig. (3) shows the cluster ionic current vs atomic mass of the clusters produced, with the main peak around 1510×10^2 a.m.u. Auger spectroscopy is carried over the 3-nm deposit and compared with that of the target. Results derived from AES (Fig. 4) show a good correlation between elemental composition of the target and that of the nanostructured Pd-Co-Mo, which implies that no significant change occur nor for the structure neither for the chemical composition of the compound. AFM analysis (Fig. 5) show high Pd-Co-Mo particle agglomeration on the membrane, which might be due to the deposition time (30-minute sample).

CONCLUSIONS

From computer calculations shown in Table 1, an estimation of the catalytic capability for a trimetallic compound might be carried to save experimental time, since its results can be used to make decisions before the synthesis of the catalytic particles. Results show that although Pt is the best catalyst for the hydrogen dissociation reaction, Pd-Co-Mo compound shows good catalytic properties too, with the compromise of lower catalytic activity.

Auger analysis (Fig. 4) show a good elemental-composition conservation while passing from the bulk material to the nanoscale structured Pd-Co-Mo, which is desired since computer calculations and estimates are based on the bulk's material structure and composition.

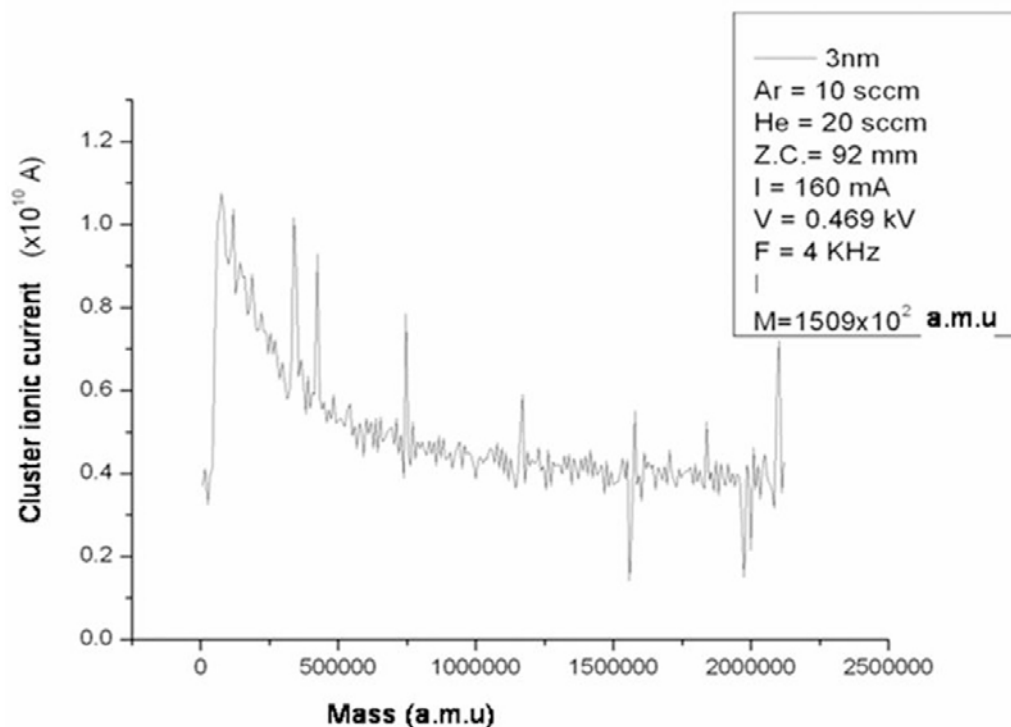


Fig. (3). 3-nm particles production curve of nanosys 500.

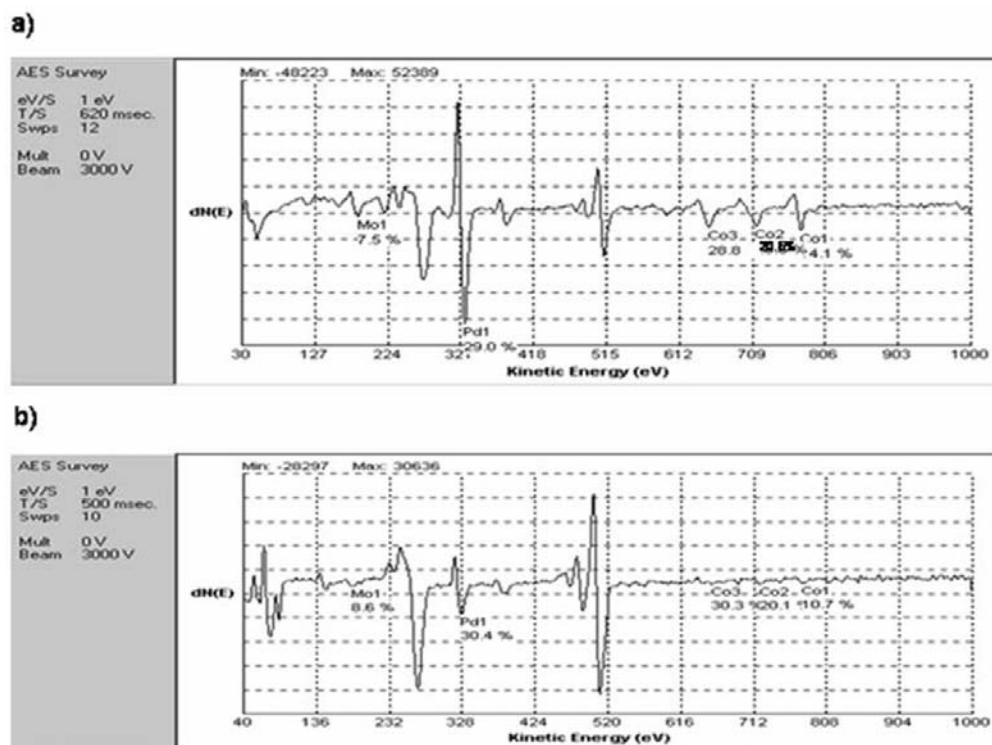


Fig. (4). AES spectra for Pd-Co-Mo: (a) target, (b) 3-nm deposit.

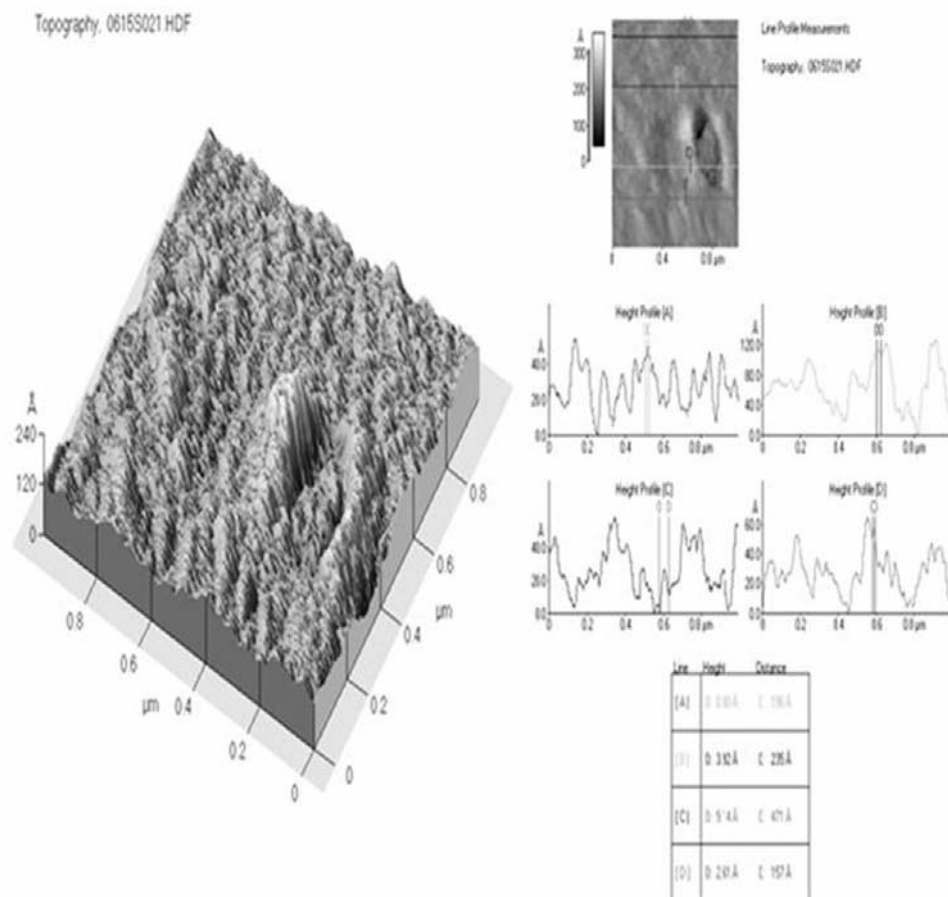


Fig. (5). AFM analysis of Pd-Co-Mo/C/nafion 112.

Reliability of calculations carried out with the use of Materials Studio software is good, although fuel cell “real life” environment is required to test the membrane’s performance.

REFERENCES

- [1] Bieberle, A. The electrochemistry of solid oxide fuel cell anodes. Diss., Technische Wissenschaften ETH Zürich, Nr. 13969. Swiss Federal Institute of Technology, Zurich, **2001**.
- [2] Kreuer, K.D. *J. Memb. Sci.*, **2001**, *185*, 29-39.
- [3] Steele, B.C.H.; Heinzel A. *Nature*, **2001**, *414*, 345-352.
- [4] Bauen, A., Hart D. *J. Power Sources*, **2000**, *86*, 482-494.
- [5] Mackerron, G. *J. Power Sources*, **2000**, *86*, 28-33.
- [6] Cacciola, G., Antonucci, V., Freni S. *J. Power Sources*, **2001**, *100*, 67-79.
- [7] Bockris, J. *Int. J. Hydrogen Energy*, **2002**, *27*, 731-740.
- [8] Ogden, J.M.; Steinbugler, M.; Kreutz, T. *J. Power Sources*, **1999**, *79*, 143-168.
- [9] Ahmed, S.; Krumpelt, M. *Int. J. Hydrogen Energy*, **2001**, *26*, 291-301.
- [10] Perry, M.L.; Fuller, T.F. *J. Electrochem. Soc.* **2002**, *149*, S59-S67.
- [11] Mathias, M.; Roth, J.; Fleming, J.; Lehnert W. *Handbook of fuel cells-fundamentals, technology and applications*, Vol. 3: Fuel cells technology and applications, John Wiley and Sons Ltd. **2003**.
- [12] Costamagna, P.; Yang, C.; Bocarsly A.B.; Srinivasan, S. *Electrochimica Acta*, **2002**, *47*, 1023-1033.
- [13] Vichi, F.M.; Colomer, M.T.; Anderson, M.A. *Electrochem. Solid-State Lett.*, **1999**, *2*(7), 313-316.
- [14] Cui, W.; Kerres, J.; Eigenberger, G. *Separat. Purif. Technol.*, **1998**, *14*, 145-154.
- [15] Genova-Dimitrova, P.; Barallie, B.; Foscallo, D.; Poinson, C.; Sánchez, J.Y. *J. Memb. Sci.*, **2001**, *185*, 59-71.
- [16] Gamburzev, S.; Appleby, A.J. *J. Power Sources*, **2002**, *107*, 5-12.
- [17] Jia, N.; Lefevre, M.C.; Halfyard, J.; Qi, Z.; Pickup, P.G., *Electrochem. Solid-State Lett.*, **2000**, *3*(12), 529-531.
- [18] Kerres, J.; Ullrich, A.; Meier, F.; Haring, T. *Solid State Ionics*, **1999**, *125*, 243-249.
- [19] Okada, T. *J. Electroanal. Chem.*, **1999**, *465*, 1-17.
- [20] Shin, S.-J.; Lee, J.-K.; Ha, H.-Y.; Hong, S.-A.; Chun, H.-S.; Oh, I.-H. *J. Power Sources*, **2002**, *106*, 146-152.
- [21] Easton, E.B.; Pickup, P.G. *Electrochem. Solid-State Lett.*, **2000**, *3*(8), 359-361.
- [22] Easton, E.B.; Qi, Z.; Kaufman, A.; Pickup, P.G., *Electrochem. Solid-State Lett.*, **2001**, *3*(5), A59-A61.
- [23] Wang, X.; Hsing, I.-M. *Electrochimica Acta*, **2002**, *47*, 2981-2987.
- [24] Maggio, G.; Recupero, V.; Pino, L. *J. Power Sources*, **2001**, *101*, 275-286.
- [25] Pisani, L.; Murgia, G.; Valentini, M.; D’aguanno, B. *J. Electrochem. Soc.*, **2002**, *149*(7), A898-A904.
- [26] Yi, J.S.; Nguyen, T.V. *J. Electrochem. Soc.*, **1999**, *146*(1), 38-45.
- [27] Andreaus, B.; McEvoy, A.J.; Scherer, G.G. *Electrochimica Acta*, **2002**, *47*, 2223-2229.
- [28] Kulikovskiy, A.A. *Electrochem. Commun.*, **2002**, *4*, 527-534.
- [29] Baldauf, M.; Preidel, W. *J. Appl. Electrochem.*, **2001**, *31*, 781-786.
- [30] Lefevre, M.C.; Martin, R.B.; Pickup, P.G. *Electrochem. Solid State Lett.*, **2001**, *2*(6), 259-261.
- [31] Löffler, M.S.; Groß, B.; Natter, H.; Hempelmann, R.; Krajewski, Th.; Divisek, J. *Phys. Chem. Chem. Phys.*, **2001**, *3*, 333-336.
- [32] Zhang, Y.; Erkey, C. *Ind. Eng. Chem. Res.*, **2005**, *44*, 5312-5317.
- [33] Subramanian, N.P.; Kumaraguru, S.P.; Colon-Mercado, H.; Kim, H.; Popov, B.N.; Black, T.; Chen, D.A. *J. Power Sources*, **2006**, *157*(1), 56-63.
- [34] Kim, H.; Popov, B.N. *Electrochem. Solid-State Lett.*, **2004**, *7*(4), A71-A74.
- [35] Cacciatore, M.; Billing, G.D. *Pure Appl. Chem.*, **1996**, *68*(5), 1075-1081.
- [36] Gross A., Department of Theoretical Chemistry, University of Ulm, <http://www.uni-ulm.de/theochem>.
- [37] Jelínek, P.; Pérez, R.; Ortega, J.; Flores, F. *Phys. Rev. Lett.*, **2006**, *96*, 046803.
- [38] Bird, D.; Humphreys, S. *Riken Rev.*, **2000**, *29*, 5-7.
- [39] Bird, D.M. *Faraday Discuss.*, **1998**, *110*, 335-346.
- [40] Truhlar, D.G.; Garrett, B.C.; Klippenstein, S. *J. Phys. Chem.*, **1996**, *100*, 12771-12800.
- [41] Raghuvver, V.; Manthiram, A.; Bard, A.J. *J. Phys. Chem. B*, **2005**, *109*(48), 22909-22912.